

Substrate-induced structures of bismuth adsorption on graphene: a first principle study

S.-Y. Lin^a, S.-L. Chang^b, H.-H. Chen,^a S. H. Su,^a J. C. A. Huang,^{a,c,d,*} M.-F. Lin^{a,*}

^aDepartment of Physics, National Cheng Kung University, Tainan 701, Taiwan.

^bDepartment of Electrophysics, National Chiao Tung University, Hsinchu 300, Taiwan.

^cAdvanced Optoelectronic Technology Center, National Cheng Kung University, Tainan 701, Taiwan.

^dTaiwan Consortium of Emergent Crystalline Materials, Ministry of Science and Technology, Taipei 106, Taiwan.

November 26, 2017

Abstract

The geometric properties of bismuth adsorbed on monolayer graphene, enriched by strong effect of substrate, are investigated by first-principle calculations. Six-layered substrate, corrugated buffer layer, and the slightly deformed monolayer graphene are all simulated. Adatom arrangements are obtained through detail analysis on adsorption energies and total energies of the various adsorption sites, revealing a hexagonal array of Bi atoms dominated by the interaction between buffer layer and monolayer graphene. Especially, bismuth clusters with periodic image is a metastable structure, which happened when bismuth atoms overcome a 50 meV energy barrier. These two kinds of structures are perfectly coincided with previous scanning tunneling microscopy measurements. The density of states are also presented, exhibiting finite value at the Fermi energy, a dip at low energy, and a shoulder structure at -0.8 eV. These primary characteristics are also found in the previous measurements of tunneling conductance.

Keywords: graphene; bismuth; first-principle; DFT

* Corresponding author. *E-mail addresses:*

jcahuang@mail.ncku.edu.tw) (J. C. A. Huang), mflin@mail.ncku.edu.tw (M.F. Lin)

1. Introduction

Two-dimensional graphene has been a mainstream material in both fundamental research and device applications since 2004, [1–3] mainly owing to its remarkable physical, chemical and material properties. [4–13] Graphene possesses a remarkable electron mobility, [4, 5] exceptionally large thermal conductivity, [6, 7] high mechanical strength, [8, 9] the anomalous quantum Hall effect, [10, 11] and the superfluidity. [12, 13] Owing to these extraordinary characteristic, graphene has attracted considerable attentions in the fields of chemistry, material science and physics. Various studies have been conducted on its electronic, [14, 15] transport, [16, 17] and magnetic [18] properties. Its essential properties can be tuned by the curvature of the structure, [19, 20] the layer numbers, [21, 22] the stacking configurations, [22, 23] the uniform or uniaxial mechanical strains, [24, 25] and the application of external electric and magnetic fields. [26, 27] This work investigates in detail how the unique substrate and buffer layer induce the feature-rich geometric properties of bismuth adsorption on graphene.

Graphene has its 2pz orbital perpendicular to its surface, providing a suitable environment to dope graphene with various elements. Numerous experimental researchers have tried to diversify the essential properties of graphene by using doping, such as O, [28, 29] H, [30, 31] N, [32, 33] transition metals, [34, 35] and heavy metals. [36, 37] Those doping elements can drastically change the electronic and magnetic properties, including semiconducting-

metal transition, the creation of magnetic moments, spintronic control, and the band gap tuning. Theoretical researchers also focus on the adatom adsorption on graphene. [38,39] Their studies on different adatom concentrations show that the electronic properties are altered dramatically under various concentration. [40] Moreover, the adatom distribution also plays an important role in tuning electronic properties even if at the same concentration. [40] Therefore, how to control the distribution of adatoms become an important issue in order to fabricate high-quality nanoelectronic devices.

Up to date, Semimetal Bi become one of the most widely studied elements due to its special physics properties. Bismuth is a Dirac fermion gas, [41] possessing long Fermi wavelength and small effective electron mass, [42] revealing narrow band gap due to strong quantum confinement effect. [43] Its low-index surfaces Bi (111), Bi (100), and Bi (110) is very different to the bulk in their electronic properties, [42] and possess less activity because they do not react much with O₂. [44] Bismuth has many possible applications in the field of environmental engineering, biochemistry, and energy storage. For example, Bi is used to detect heavy metals, [45] and bismuth oxide can be a biosensor [46] or a anode of lithium battery. [47] On the other hand, some theoretical study are performed with the calculation of geometric and electronic properties of Bi interact with graphene. [48,49] However, the distribution of Bi atoms and the effect of substrate are still not well understood.

In this paper, how to create the different bismuth distribution via the effect of substrate is investigated by first principle calculations. This work shows the adsorption energy of

various atomic sites, including hollow site, top site, and bridge site. The calculation results are further enhanced by analyzing the total energy of various position in the graphene surface, which provide the strong evidence of energetic favorable adsorption site of bismuth. This directly reflect the effect of non-uniform Van der Waals interactions between buffer layer and monolayer graphene. Moreover, the effect of bismuth on density of states (DOS) could be understood by a thorough comparison with experimental measurements of tunneling conductance. [50, 51] All the calculated geometric structures are compare with scanning tunneling microscopy (STM) measurements in detail. [50, 51] Hopefully, these rich fundamental features in bismuth structures can promote potential applications in electronic devices or energy materials.

2. Methods

Our first-principle calculations are based on the density functional theory (DFT) implemented by the Vienna *ab initio* simulation package (VASP). [52] The generalized gradient approximation (GGA), within the Perdew-Burke-Ernzerhof (PBE) functional, [53] is applied to describe the exchange-correlation energy of interacting electrons, and the projector augmented wave (PAW) is utilized to describe the electron-ion interactions. The van der Waals (vdW) force is employed in the calculations using the semiempirical DFT-D2 correction of Grimme to correctly describe the atomic interactions between graphene layers. [54] A vacuum space of 15 angstroms is inserted between periodic images to avoid interactions,

and the cutoff energies of the wave function expanded by plane waves were chosen to be 400 eV. For calculations of the electronic properties and the optimal geometric structures, the first Brillouin zones are sampled by $3 \times 3 \times 1$ k -points via the Monkhorst-Pack scheme. The convergence of the Hellmann-Feynman force is set to 0.01 eV \AA^{-1} .

3. Results and discussion

First, in order to accurately simulate the bismuth adsorbed on monolayer graphene, we start from the six-layer Si-terminated 4H-SiC (0001) substrate. The optimized results show that the four layer structure (region I in Fig. 1), which reduced from six-layer substrate has their geometric properties almost the same. Second, a buffer layer, as shown in region II of Fig. 1, is in a periodic bubble shape after relaxation, in which their troughs bond with silicon atoms of the substrate. This buffer layer, when compared with previous STM measurements, is very close in their periodic corrugation. Third, the monolayer graphene is nearly flat with its C-C bond length at 1.50 \AA , as shown in the region III. The distance between monolayer graphene and buffer layer is varies from 3.21 to 5.45 at the crests and troughs. Such difference directly influence the Van der Waals interactions between the two layers, and will plays an important role in the distribution of bismuth. Finally, bismuth atoms can adsorb on monolayer graphene after self-consistent calculation (region IV in Fig. 1). There are several kinds of distribution of bismuth atoms based on different experiment environments, such as most uniformed distribution and bismuth clusters, which depending

on their adsorption energy.

The adsorption energy ΔE , characterizing the reduced energy owing to the bismuth atoms adsorbed on graphene, is very useful to understand the stability of adsorbed atoms.

It is defined as

$$\Delta E = E_{Total} - E_{Gra} - E_{Buf} - E_{Bi}, \quad (1)$$

where E_{Total} , E_{Gra} , E_{Buf} , and E_{Bi} are the total energies of the system, pristine graphene monolayer, buffer layer, and isolated bismuth atoms, respectively. The adsorption energies of different adsorption sites of bismuth atoms on graphene are present in table 1. Three adsorption sites with higher geometric symmetry are investigated, including hollow, bridge, and top site. The bismuth atom on the hollow site of the carbon hexagon has the lowest adsorption energy, directly illustrated its less stable configuration. The other two cases, bridge site and top site, have similar adsorption energy, while the bridge site possesses the highest adsorption energy. This indicates that bismuth atoms are most possible to be found at bridge site. Moreover, the distance h between bismuth and graphene surface corresponding to various adsorption sites is also calculated. The shorter distance of bridge sites indicates the stronger interaction between bismuth atoms and graphene, and this also accounts for its stability.

The distribution of bismuth atoms can be investigated in detail by calculating the total energy. Based on our former discussion, bridge site is the much stable site within

Table 1: Adsorption energy for various site.

Site	$\Delta E(\text{eV})$	$h (\text{\AA})$
H	0.6602	2.51
B	1.3450	2.32
T	1.2904	2.34

a single hexagonal. The total energy of the bridge site along the periodic direction are all calculated, which is very helpful to understand the most stable position in monolayer graphene, as shown in Fig. 2. The red hexagonal region has the most closest distance to buffer layer (at about 3.21 \AA), and its total energy is the lowest among all bridge site. This energy is defined as zero in order to compare with other bridge site. A bit away from the red hexagonal, the bridge sites between red and yellow stick have higher total energies. Their energy differences is about 17 23 meV. As for the other parts with grey hexagonal, possessing comparable total energy to each other, exhibit the highest total energy difference at about 50 meV. This indicates that the bismuth atoms is hardly transport to other region, i.e., it is most stable at the red hexagonal. The fact that the energy barrier (50 meV) is larger than that at the room temperature (25 meV) being the main reason. It is noticed that the Van der Waals interactions between the red hexagonal and the crest of buffer layer is the strongest part in graphene surface, being the origination of above-mentioned stability.

Based on the former analysis of adsorption energy and total energy, the large-scale

pattern of bismuth can be discuss in detail. The periodic image of monolayer graphene is shown in Fig. 3(a), where the red and grey region represent the most stable and unstable site, respectively. The shortest interatomic distance of Bi atoms can be 14 Å, which is the closest distance between each red sticks. The opposite is true for the longest distance 18 Å, and the average distance is 15.9 Å. This indicates the most possible distance between two bismuth is within 14 18 Å. The previous STM experimental measurements, [50, 51] revealing the distribution of bismuth atoms, are worth to compare with our simulations. Fig. 3 presents a large-scale hexagonal array of Bi atoms, and the interatomic distance of more than 60% Bi atoms is 15 and 16 Å, while some Bi atoms (30%) have their Bi-Bi distance at 14 and 17 Å. All the simulation results agree with these STM measurements. This further illustrate that periodic corrugation of buffer layer do influence the monolayer graphene, and thus the arrangement of bismuth.

Besides the most stable structure, there may exists certain metastable structures due to various experiment environment. Previous experiments [51] reveal a structure with several bismuth clusters that formed by some bismuth atoms, as shown in Fig. 4(a). We simulate many possibilities, obtaining the most possible structure with three bismuth cluster, as indicates in Fig. 4(b). These Bi atoms is arranged in triangle pattern with each of them posit at the bridge site of a single hexagonal. There interatomic distance is 2.88 Å, which is a suitable distance to prevent the repulsive force from each other. It is noticed that in order to form this pattern, the bismuth atom from the above-mentioned large-scale hexagonal

need to overcome the energy barrier (50 meV in Fig. 2). This can perfectly explain why this special pattern appear after heating and annealing process. Moreover, the distance between two bismuth clusters is about 16 Å, which demonstrate that energetic favorable adsorption site of those bismuth clusters is the red hexagonal (Fig. 2). This further clarify that the effects of buffer layer still plays an important role after heating and annealing.

The density of states (DOS) can directly reflects the primary electronic properties of the system. For hexagonal array of Bi atoms adsorbed graphene, DOS is finite at the Fermi level ($E_F = 0$); it possesses a dip at low energy, and a shoulder structure at $E \sim -0.8$ eV, as shown in Fig. 5(a). The finite value at $E_F = 0$ illustrates that there exists certain amount of free carriers. The dip at about -0.2 eV is ascribed to the Dirac point, indicating that bismuth atoms introduce n-type doping in the system. The shoulder structure at $E \sim -0.8$ eV comes from the bismuth atoms contribution. Such states can be a characteristic to identify the existence of bismuth atoms. The STS measurements, in which the tunneling differential conductance map of the dI/dV - V curve is proportional to DOS, can provide an accurate and efficient way to examine theoretical calculation. Previous experiments [50,51] exhibit the similar feature to the DFT calculation, as shown in Fig. 5(b). The finite DOS at $E_F = 0$ and the small dip at low energy show a good agreement with theoretical results. The peak at -0.7 eV originates from the bismuth atoms is similar to the shoulder structure in our calculation. The above-mentioned comparison in electronic properties might promote potential applications in electronic devices.

4. Conclusion

The geometric and electronic properties of bismuth adsorbed on monolayer graphene are investigated by *ab initio* density functional theory calculations. Calculations of the adsorption energies and total energies with various adsorption sites of bismuth atoms are performed. Geometric properties are enriched by substrate and buffer layer, in which the rippled buffer layer are the critical factor affecting the bismuth distributions. Remarkably, four-layer Si-terminated 4H-SiC (0001) substrate structures are obtained, leading to periodic corrugated buffer layer. Such buffer layer create a periodic potential to the graphene monolayer, resulting in uniformly distributed bismuth arrangement. Two kinds of different bismuth distribution are obtained by analyzing the total energy and energy barrier of the system, including hexagonal array of Bi atoms and bismuth clusters arranged in triangle pattern, where the later belong to a metastable structure. These geometric properties can be tune by different experiment environment, including heating and annealing. Both of the two patterns are in a great agreement with previous experimental results. The density of states of graphene with hexagonal bismuth array can exhibit its primary electronic properties, revealing finite DOS at the Fermi level, a dip structure at low energy, and a shoulder structure at $E \sim -0.8$ eV. These can be an important evidence to validate the existence of n-type doping by bismuth, Dirac cone structure, and the bismuth contributed states. A comparison of density of states between theoretical and experimental results are performed,

which the tunneling conductance making a good coincidence with DOS in their primary feature. These tunable geometric structure and features-rich electronic properties may be potentially important for the applications of bismuth adsorbed systems in nanoelectronic devices.

Acknowledgments

This work was supported by the Physics Division, National Center for Theoretical Sciences (South), the Nation Science Council of Taiwan (Grant No. NSC 102-2112-M-006-007-MY3). We also thank the National Center for High-performance Computing (NCHC) for computer facilities.

References

- [1] Novoselov, Kostya S., et al. "Electric field effect in atomically thin carbon films." science 306.5696 (2004): 666-669.
- [2] Geim, Andre K., and Konstantin S. Novoselov. "The rise of graphene." Nature materials 6.3 (2007): 183-191.
- [3] Novoselov, K. S. A., et al. "Two-dimensional gas of massless Dirac fermions in graphene." nature 438.7065 (2005): 197-200.
- [4] Orlita, Milan, et al. "Approaching the Dirac point in high-mobility multilayer epitaxial graphene." Physical review letters 101.26 (2008): 267601.
- [5] Wang, Shuai, et al. "High mobility, printable, and solution-processed graphene electronics." Nano letters 10.1 (2009): 92-98.
- [6] Balandin, Alexander A., et al. "Superior thermal conductivity of single-layer graphene." Nano letters 8.3 (2008): 902-907.
- [7] Barbarino, Giuliana, Claudio Melis, and Luciano Colombo. "Intrinsic thermal conductivity in monolayer graphene is ultimately upper limited: A direct estimation by atomistic simulations." Physical Review B 91.3 (2015): 035416.
- [8] Lee, Changgu, et al. "Measurement of the elastic properties and intrinsic strength of monolayer graphene." science 321.5887 (2008): 385-388.

- [9] Vadukumpully, Sajini, et al. "Flexible conductive graphene/poly (vinyl chloride) composite thin films with high mechanical strength and thermal stability." *Carbon* 49.1 (2011): 198-205.
- [10] Zhang, Yuanbo, et al. "Experimental observation of the quantum Hall effect and Berry's phase in graphene." *Nature* 438.7065 (2005): 201-204.
- [11] Novoselov, K. S., et al. "Unconventional quantum Hall effect and Berrys phase of 2k in bilayer graphene." *Nature physics* 2.3 (2006): 177-180.
- [12] Min, Hongki, et al. "Room-temperature superfluidity in graphene bilayers." *Physical Review B* 78.12 (2008): 121401.
- [13] Perali, Andrea, David Neilson, and Alex R. Hamilton. "High-temperature superfluidity in double-bilayer graphene." *Physical review letters* 110.14 (2013): 146803.
- [14] Neto, AH Castro, et al. "The electronic properties of graphene." *Reviews of modern physics* 81.1 (2009): 109.
- [15] Ohta, Taisuke, et al. "Controlling the electronic structure of bilayer graphene." *Science* 313.5789 (2006): 951-954.
- [16] Hwang, E. H., S. Adam, and S. Das Sarma. "Carrier transport in two-dimensional graphene layers." *Physical Review Letters* 98.18 (2007): 186806.

- [17] Sarma, S. Das, et al. "Electronic transport in two-dimensional graphene." *Reviews of Modern Physics* 83.2 (2011): 407.
- [18] Xiao, Di, Wang Yao, and Qian Niu. "Valley-contrasting physics in graphene: magnetic moment and topological transport." *Physical Review Letters* 99.23 (2007): 236809.
- [19] Guinea, F., M. I. Katsnelson, and M. A. H. Vozmediano. "Midgap states and charge inhomogeneities in corrugated graphene." *Physical Review B* 77.7 (2008): 075422.
- [20] Lin, Shih-Yang, et al. "Feature-rich electronic properties in graphene ripples." *Carbon* 86 (2015): 207-216.
- [21] Sutter, P., et al. "Electronic structure of few-layer epitaxial graphene on Ru (0001)." *Nano letters* 9.7 (2009): 2654-2660.
- [22] Hao, Yufeng, et al. "Probing Layer Number and Stacking Order of Few-Layer Graphene by Raman Spectroscopy." *Small* 6.2 (2010): 195-200.
- [23] Wu, Jhao-Ying, Godfrey Gumbs, and Ming-Fa Lin. "Combined effect of stacking and magnetic field on plasmon excitations in bilayer graphene." *Physical Review B* 89.16 (2014): 165407.
- [24] Guinea, F., M. I. Katsnelson, and A. K. Geim. "Energy gaps and a zero-field quantum Hall effect in graphene by strain engineering." *Nature Physics* 6.1 (2010): 30-33.

- [25] Wong, Jen-Hsien, Bi-Ru Wu, and Ming-Fa Lin. "Strain effect on the electronic properties of single layer and bilayer graphene." *The Journal of Physical Chemistry C* 116.14 (2012): 8271-8277.
- [26] Castro, Eduardo V., et al. "Biased bilayer graphene: semiconductor with a gap tunable by the electric field effect." *Physical Review Letters* 99.21 (2007): 216802.
- [27] Lai, Y. H., et al. "Magnetoelectronic properties of bilayer Bernal graphene." *Physical Review B* 77.8 (2008): 085426.
- [28] Ito, Jun, Jun Nakamura, and Akiko Natori. "Semiconducting nature of the oxygen-adsorbed graphene sheet." *Journal of applied physics* 103.11 (2008): 113712.
- [29] Ryu, Sunmin, et al. "Atmospheric oxygen binding and hole doping in deformed graphene on a SiO₂ substrate." *Nano letters* 10.12 (2010): 4944-4951.
- [30] Elias, D. C., et al. "Control of graphene's properties by reversible hydrogenation: evidence for graphane." *Science* 323.5914 (2009): 610-613.
- [31] Ryu, Sunmin, et al. "Reversible basal plane hydrogenation of graphene." *Nano letters* 8.12 (2008): 4597-4602.
- [32] Qu, Liangti, et al. "Nitrogen-doped graphene as efficient metal-free electrocatalyst for oxygen reduction in fuel cells." *ACS nano* 4.3 (2010): 1321-1326.

- [33] Yeh, Te-Fu, et al. "Nitrogen-Doped Graphene Oxide Quantum Dots as Photocatalysts for Overall Water-Splitting under Visible Light Illumination." *Advanced Materials* 26.20 (2014): 3297-3303.
- [34] Krasheninnikov, A. V., et al. "Embedding transition-metal atoms in graphene: structure, bonding, and magnetism." *Physical review letters* 102.12 (2009): 126807.
- [35] Pi, K., et al. "Electronic doping and scattering by transition metals on graphene." *Physical Review B* 80.7 (2009): 075406.
- [36] Machida, Motoi, Tomohide Mochimaru, and Hideki Tatsumoto. "Lead (II) adsorption onto the graphene layer of carbonaceous materials in aqueous solution." *Carbon* 44.13 (2006): 2681-2688.
- [37] Marchenko, D., et al. "Giant Rashba splitting in graphene due to hybridization with gold." *Nature communications* 3 (2012): 1232.
- [38] Chan, Kevin T., J. B. Neaton, and Marvin L. Cohen. "First-principles study of metal adatom adsorption on graphene." *Physical Review B* 77.23 (2008): 235430.
- [39] Khomyakov, P. A., et al. "First-principles study of the interaction and charge transfer between graphene and metals." *Physical Review B* 79.19 (2009): 195425.
- [40] Balog, Richard, et al. "Bandgap opening in graphene induced by patterned hydrogen adsorption." *Nature materials* 9.4 (2010): 315-319.

- [41] Li, Lu, et al. "Phase transitions of Dirac electrons in bismuth." *Science* 321.5888 (2008): 547-550.
- [42] Hofmann, Ph. "The surfaces of bismuth: Structural and electronic properties." *Progress in surface science* 81.5 (2006): 191-245.
- [43] Black, M. R., et al. "Infrared absorption in bismuth nanowires resulting from quantum confinement." *Physical Review B* 65.19 (2002): 195417.
- [44] Bobaru, S., et al. "Competing allotropes of Bi deposited on the Al₁₃Co₄ (100) alloy surface." *Physical Review B* 86.21 (2012): 214201.
- [45] Wanekaya, Adam K. "Applications of nanoscale carbon-based materials in heavy metal sensing and detection." *Analyst* 136.21 (2011): 4383-4391.
- [46] Shan, Dan, et al. "Polycrystalline bismuth oxide films for development of amperometric biosensor for phenolic compounds." *Biosensors and Bioelectronics* 24.12 (2009): 3671-3676.
- [47] Li, Yuling, et al. "Bismuth oxide: a new lithium-ion battery anode." *Journal of Materials Chemistry A* 1.39 (2013): 12123-12127.
- [48] Akturk, Olcay Uzengi, and Mehmet Tomak. "Bismuth doping of graphene." *Applied Physics Letters* 96.8 (2010): 081914.

- [49] Hsu, Chia-Hsiu, Vidvuds Ozolins, and Feng-Chuan Chuang. "First-principles study of Bi and Sb intercalated graphene on SiC (0001) substrate." *Surface Science* 616 (2013): 149-154.
- [50] Chen, H-H., et al. "Long-range interactions of bismuth growth on monolayer epitaxial graphene at room temperature." *Carbon* 93 (2015): 180-186.
- [51] Chen, H-H., et al. "Tailoring low-dimensional structures of bismuth on monolayer epitaxial graphene." *Scientific reports* 5 (2015).
- [52] Kresse, Georg, and Jurgen Furthmuller. "Efficient iterative schemes for ab initio total-energy calculations using a plane-wave basis set." *Physical Review B* 54.16 (1996): 11169.
- [53] Perdew, John P., Kieron Burke, and Matthias Ernzerhof. "Generalized gradient approximation made simple." *Physical review letters* 77.18 (1996): 3865.
- [54] Grimme, Stefan. "Semiempirical GGA-type density functional constructed with a long-range dispersion correction." *Journal of computational chemistry* 27.15 (2006): 1787-1799.

FIGURE CAPTIONS

Fig. 1. Geometric structure of silicon carbide substrate, buffer layer, monolayer graphene, and bismuth adatoms.

Fig. 2. Total energies of bismuth adsorption on different position of monolayer graphene.

Fig. 3. Geometric structures of hexagonal array of Bi atoms of (a) DFT calculation and (b) STM measurement.

Fig. 4. Geometric structures of bismuth clusters of (a) DFT calculation and (b) STM measurement.

Fig. 5. Densities of states of hexagonal array of Bi atoms of (a) DFT calculation and (b) STM measurement.

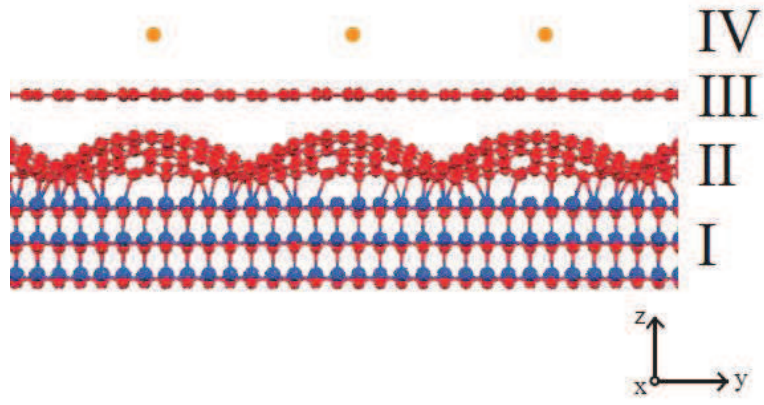


Figure 1: Geometric structure of silicon carbide substrate, buffer layer, monolayer rgaphene, and bismuth adatoms.

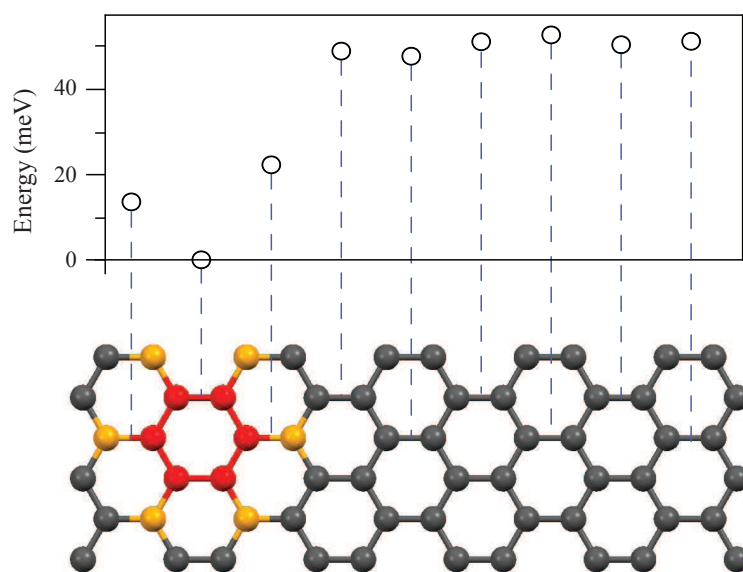
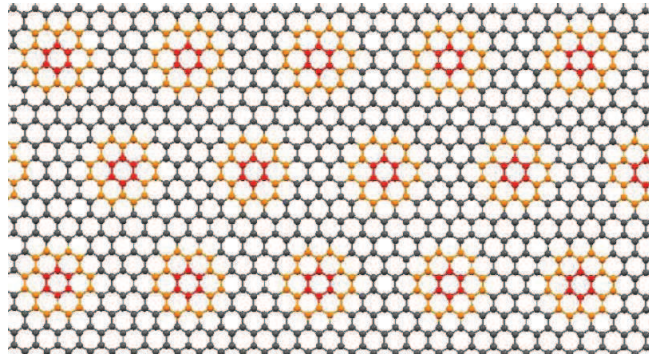


Figure 2: Total energies of bismuth adsorption on different position of monolayer graphene.

(a)



(b)

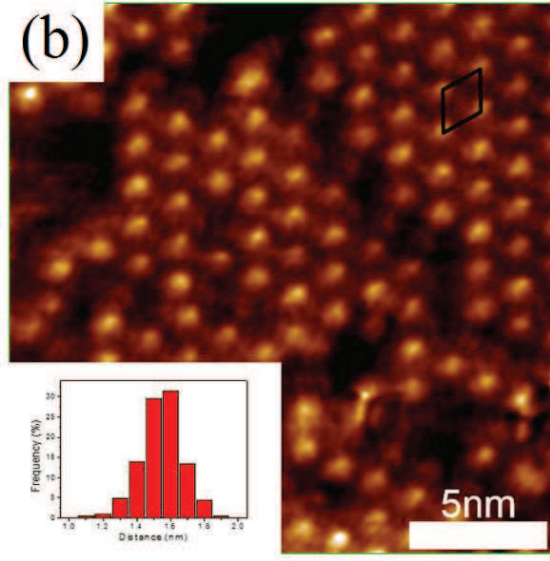
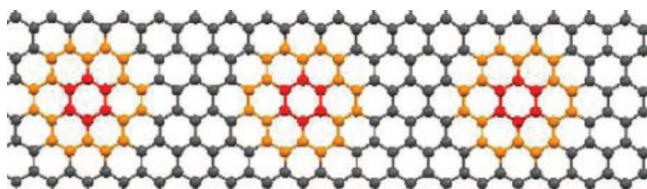


Figure 3: Geometric structures of hexagonal array of Bi atoms of (a) DFT calculation and (b) STM measurement.

(a)



(b)

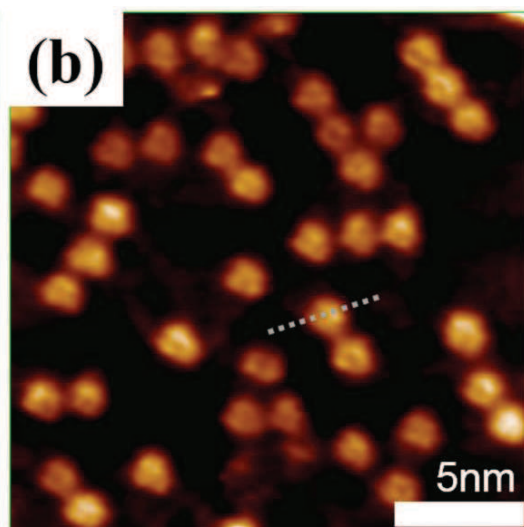


Figure 4: Geometric structures of bismuth clusters of (a) DFT calculation and (b) STM measurement.

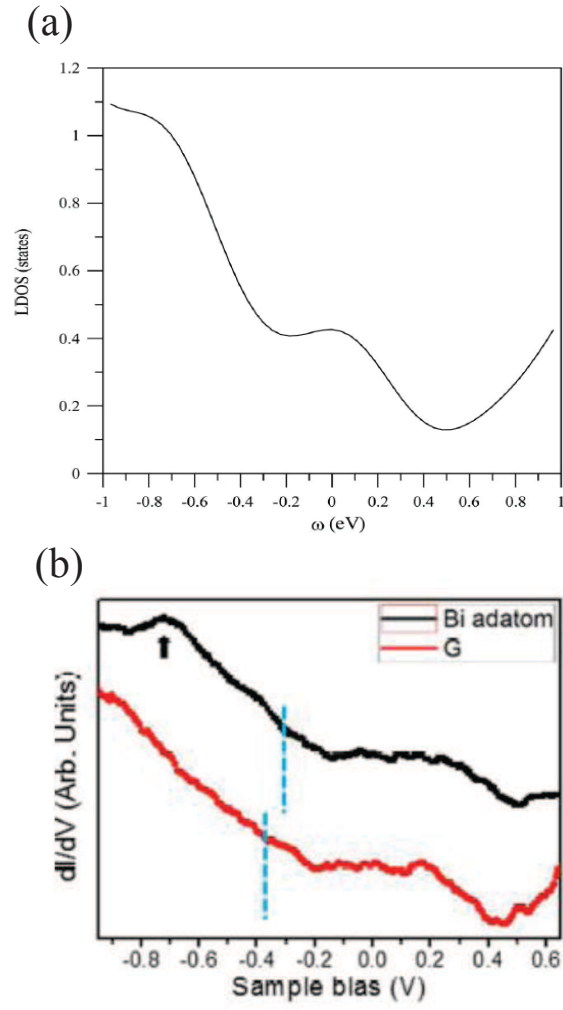


Figure 5: (a) Densities of states of DFT calculation and (b) tunneling conductance of STS measurement of bismuth hexagonal array system.